Joint Location and Beamforming Optimization for STAR-RIS Aided NOMA-UAV Networks

Yuhua Su, Xiaowei Pang, Weidang Lu, *Senior Member, IEEE,* Nan Zhao, *Senior Member, IEEE,* Xianbin Wang, *Fellow, IEEE* and Arumugam Nallanathan, *Fellow, IEEE*

***Abstract*—This work investigates the potential of combining unmanned aerial vehicle (UAV) and simultaneously transmitting and reflecting reconfigurable intelligent surface (STAR-RIS) in wireless networks. In particular, the signals from UAV can be reflected and transmitted through STAR-RIS to the users on both sides of the surface to provide full-space coverage. We formulate a sum-rate maximization problem in STAR-RIS aided non-orthogonal multiple access UAV networks, where the location and power allocation of UAV, and the passive reflection/transmission beamforming of STAR-RIS are jointly optimized, subject to the quality-of-service requirement. Furthermore, we transform the non-convex problem into a convex one and propose an efficient algorithm to obtain the suboptimal solution to the original problem. Simulation results verify the superiority of the proposed scheme compared to other benchmarks.**

***Index Terms*—Non-orthogonal multiple access, reconfigurable intelligent surface, simultaneous transmission and reflection, unmanned aerial vehicle.**

I. Introduction

Reconfigurable intelligent surface (RIS) has been envisioned as a promising technology for future wireless networks [1]. Specifically, each element of RIS, which is made of electromagnetic material and metal patches, can reflect the incident signal by altering its phase shift intelligently [2]. Thus, the wireless propagation environment can be reshaped through collaboratively adjusting the phase shifts of massive reflecting elements. With the advantages of easy deployment, low energy consumption and low hardware cost, RIS has been widely studied in industry and academia to improve the achievable rate, security and reliability [3].

On the other hand, unmanned aerial vehicles (UAVs) have been extensively utilized in wireless networks owing to their low cost, high mobility and line-of-sight (LoS) transmission [4]. In [5], Wang *et al.* studied a UAV-enabled relay system to maximize the sum harvested energy of users. To efficiently utilize the mobility of UAV, Yuan *et al.* introduced artificial potential filed to propose a novel optimal trajectory design method in [6]. However, the UAV-ground channel may be blocked in the urban environment, which is a challenging issue. By introducing RIS into UAV communication, additional advantages can be gained to reconfigure the air-ground channels, thereby significantly improving the communication quality [7], [8]. Pang *et al.* in [9] integrated UAV and RIS to facilitate the security in wireless networks. In [10], Mei *et al.* maximized the energy efficiency by jointly optimizing the three-dimensional (3D) space of UAV and phase shifts of RIS. However, it is noteworthy that the RIS deployed on the facades of buildings can only reflect signals to the users located on the same side, which limits the coverage [11].

To deal with this challenging issue, the RIS that can simultaneously enable transmission and reflection (STAR-RIS) has emerged [12]. Some promising technologies and successful prototypes have been conducted for the practical implementation of STAR-RIS [13]. Compared to the conventional RIS, the users located in the back side of STAR-RIS can be also served to realize full-space coverage. Meanwhile, by adjusting the phase shifts and power ratio of the reflected and transmitted signals, STAR-RIS can construct favorable propagation environments for the users of both sides. Accordingly, the potential of combining UAV and STAR-RIS to improve the performance is worth investigating. In [14], Liu *et al.* introduced STAR-RIS into UAV networks to maximize the rate by jointly optimizing the trajectory and phase shifts. The UAV trajectory was jointly optimized by Zhang *et al.* with power allocation and STAR-RIS's passive beamforming in [15] to maximize the sum rate.

In STAR-RIS aided UAV networks, the trajectory optimization may become ineffective, due to the delayed and unreliable channel state information (CSI) caused by fading. Motivated by this, in this correspondence, the UAV's location is jointly optimized with the transmit power and transmission/reflection beamforming based on the hovering characteristic of rotary-wing UAVs, without acquiring offline/online CSI for trajectory planning. We aim at enhancing the sum rate of non-orthogonal multiple access (NOMA) UAV network subject to quality of service (QoS) requirements. An iterative algorithm is developed to solve the joint optimization problem effectively.

II. System model

Consider a downlink NOMA-UAV network, where a single-antenna UAV connects with two single-antenna users with

Manuscript received September 27, 2022; revised January 13 and March 10, 2023; accepted March 21, 2023. The work was supported by the National Natural Science Foundation of China (NSFC) under Grant 62271099 and 62271447. The associate editor coordinating the review of this paper and approving it for publication was Y. Hu. *(Corresponding author: Nan Zhao.)*

Y. Su, X. Pang and N. Zhao are with the Key Laboratory of Intelligent Control and Optimization for Industrial Equipment of Ministry of Education, Dalian University of Technology, Dalian 116024, P. R. China (email: suyuhua@mail.dlut.edu.cn, xiaoweipang00@mail.dlut.edu.cn, zhaonan@dlut.edu.cn).

Weidang Lu is with the College of Information Engineering, Zhejiang University of Technology, Hangzhou 310023, China (e-mail: luweid@zjut.edu.cn).

Xianbin Wang is with the Department of Electrical and Computer Engineering, Western University, London, ON N6A 5B9, Canada (e-mail: xianbin.wang@uwo.ca).

A. Nallanathan is with the School of Electronic Engineering and Computer Science, Queen Mary University of London, London E1 4NS, U.K. (e-mail: a.nallanathan@qmul.ac.uk).

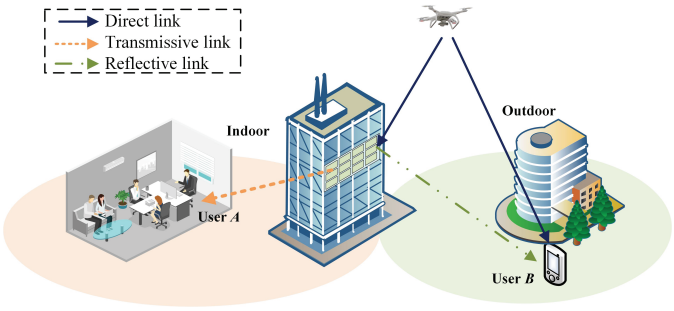

Fig. 1. STAR-RIS aided NOMA-UAV network.

the assistance of STAR-RIS. The users are denoted by U_i, $i \in \mathcal{I} = \{A, B\}$. As shown in Fig. 1, the incident signal is reconfigured by the STAR-RIS, and then transmitted to the indoor User A and simultaneously reflected to the outdoor User B. Assume that the RIS is composed of a uniform planar array (UPA) with M elements. For simplicity, we adopt the same transmission and reflection coefficients for all the STAR-RIS elements. Define $\mathbf{\Phi}_A = \sqrt{\beta_A}\text{diag}(e^{j\theta_A^1}, \cdots, e^{j\theta_A^M}) = \sqrt{\beta_A}\mathbf{\Theta}_A$ and $\mathbf{\Phi}_B = \sqrt{\beta_B}\text{diag}(e^{j\theta_B^1}, \cdots, e^{j\theta_B^M}) = \sqrt{\beta_B}\mathbf{\Theta}_B$ as the transmission and reflection beamforming matrices, where β_i and θ_i^m are the transmission/reflection coefficients and phase-shift adjustment of the mth element, respectively[1]. Owing to the law of energy conservation, $\beta_A + \beta_B = 1$.

3D Cartesian coordinate system is adopted, where the coordinate of U_i is denoted as $\mathbf{q}_i = [x_i, y_i, z_i]$. The STAR-RIS and UAV are respectively located at $\mathbf{q}_I = [x_I, y_I, z_I]$ and $\mathbf{Q} = [x_U, y_U, H]$, where the UAV is assumed to hover at a fixed height H. Denote $\mathbf{h}_{UI} \in \mathbb{C}^{M\times 1}$ and $\mathbf{h}_{Ii} \in \mathbb{C}^{1\times M}$ as the channels from UAV to RIS and from RIS to users, which can be modeled as LoS and expressed as

$$\mathbf{h}_{UI} = \sqrt{\rho d_{UI}^{-2}}\tilde{\mathbf{h}}_{UI}, \tag{1}$$

$$\mathbf{h}_{Ii} = \sqrt{\rho d_{Ii}^{-2}}\tilde{\mathbf{h}}_{Ii}, i = A, B, \tag{2}$$

where ρ is the channel gain at the reference distance of 1 m, and $d_{UI} = \sqrt{\|\mathbf{q}_I - \mathbf{Q}\|^2}$ and $d_{Ii} = \sqrt{\|\mathbf{q}_I - \mathbf{q}_i\|^2}$ are the distance between UAV and RIS and that between RIS and U_i, respectively. $\tilde{h}_{UI}$ and $\tilde{h}_{Ii}$ are the array responses of STAR-RIS when the signal arrive at and depart from RIS, respectively. Denote $h_{UB} \in \mathbb{C}^{1\times 1}$ as the direct link between UAV and U_B, which is blocked and modeled by Rayleigh fading as

$$h_{UB} = \sqrt{\rho d_{UB}^{-\alpha}}\tilde{h}, \tag{3}$$

where $d_{UB} = \sqrt{\|\mathbf{Q} - \mathbf{q}_B\|^2}$ is the distance between the UAV and U_B, $\alpha \geq 2$ is the path-loss exponent and $\tilde{h} \sim \mathcal{CN}(0, 1)$. As the UAV-RIS-user channel is dominated by the LoS component and the UAV is hovering at the fixed location, we assume that the perfect CSI can be obtained with existing channel estimation techniques [17].

The superposed information is transmitted from the UAV to users via NOMA. Accordingly, the received signals at U_i can be expressed as

[1]We consider the metasurface-based implementation, and its independent phase-shift control can serve as an upper bound of the coupled phase-shift model [16], which is worth pursuing in the future.

$$y_A = (\mathbf{h}_{IA}\mathbf{\Phi}_A\mathbf{h}_{UI})(\sqrt{p_A}s_A + \sqrt{p_B}s_B) + n_A, \tag{4}$$

$$y_B = (\mathbf{h}_{IB}\mathbf{\Phi}_B\mathbf{h}_{UI} + h_{UB})(\sqrt{p_A}s_A + \sqrt{p_B}s_B) + n_B, \tag{5}$$

where p_i is the transmit power allocated to U_i, s_i denotes the transmitted signal for U_i, and $n_i \sim \mathcal{CN}(0, \sigma^2)$ denotes the additive white Gaussian noise at U_i.

Assume that the successive interference cancellation (SIC) order is $U_B \to U_A$. According to NOMA, we first decode the signal of U_B by treating the signal of U_A as noise, and then remove it from the superposed signal. The achievable rate of U_i can be given by

$$R_A = \log_2(1 + \text{SINR}_A), \tag{6}$$

$$R_B = \min\{\log_2(1 + \text{SINR}_B^1), \log_2(1 + \text{SINR}_B^2)\}. \tag{7}$$

Define the channel gains of U_A and U_B as $\mathbf{H}_A = \|\mathbf{h}_{IA}\mathbf{\Phi}_A\mathbf{h}_{UI}\|^2$ and $\mathbf{H}_B = \|\mathbf{h}_{IB}\mathbf{\Phi}_B\mathbf{h}_{UI} + h_{UB}\|^2$, respectively. The signal-to-interference-plus-noise ratio (SINR) of signal s_A at U_A can be expressed as

$$\text{SINR}_A = \frac{p_A\mathbf{H}_A}{\sigma^2}, \tag{8}$$

and the SINR to decode s_B at U_B and U_A can be respectively expressed as

$$\text{SINR}_B^1 = \frac{p_B\mathbf{H}_B}{p_A\mathbf{H}_B + \sigma^2}, \quad \text{SINR}_B^2 = \frac{p_B\mathbf{H}_A}{p_A\mathbf{H}_A + \sigma^2}. \tag{9}$$

III. Problem Formulation

We aim at maximizing the sum rate via jointly optimizing the power allocation, the transmission and reflection beamforming and the hovering location, subject to QoS requirements. Since U_B owns a much longer distance with UAV, leading to a poor quality of the UAV-U_B channel, we assume that the channel quality of U_A is better than that of U_B, i.e., $\mathbf{H}_A \geq \mathbf{H}_B$. Accordingly, the achievable rate of U_B can be expressed as $R_B = \log_2(1 + \text{SINR}_B^1)$. Thus, the problem can be formulated as

$$\max_{\mathbf{\Phi_i}, p_i, \mathbf{Q}} \quad R_A + R_B \tag{10a}$$

$$s.t. \quad 0 \leq \theta_i^m < 2\pi, \forall i, m, \tag{10b}$$

$$\beta_A + \beta_B = 1, \tag{10c}$$

$$p_A + p_B = p, \tag{10d}$$

$$p_A \leq p_B, \tag{10e}$$

$$\text{SINR}_A \geq \gamma_A, \tag{10f}$$

$$\text{SINR}_B^1 \geq \gamma_B, \tag{10g}$$

$$\mathbf{H}_A \geq \mathbf{H}_B, \tag{10h}$$

$$\mathbf{Q} \in \mathbf{L}, \tag{10i}$$

where p is the total transmit power of UAV, $\mathbf{Q}$ denotes the UAV location, and $\mathbf{L}$ is the area where the UAV can hover. It is challenging to solve it due to the non-convex constraints and coupled variables.

IV. Proposed Solutions

In this section, we decompose (10) into two sub-problems based on the block coordinate descent (BCD) method, and an iterative algorithm is proposed to solve them alternatively.

A. Joint Optimization of $\mathbf{\Phi}_i$ and p_i

With the given UAV location $\mathbf{Q}$, the sub-problem can be formulated as

$$\max_{\boldsymbol{\Theta_i},\beta_i,p_i,} \quad \log_2\left(1+\frac{p_A\mathbf{H}_A}{\sigma^2}\right)+\log_2\left(1+\frac{p_B\mathbf{H}_B}{p_A\mathbf{H}_B+\sigma^2}\right) \tag{11a}$$

$$s.t. \quad (10b)-(10h). \tag{11b}$$

Note that the STAR-RIS allows for independent optimization of phase shifts of the transmitted and reflected signals. First, we have the following lemma for the closed-form solution to $\boldsymbol{\Theta}_A$.

Lemma 1: With other variables fixed, the optimal phase-shift of STAR-RIS for the transmitted signal can be given by

$$\theta_A^{m*} = \theta^* - \text{angle}\{W_m\}, \tag{12}$$

where W_m is the mth value of $\mathbf{W} = \text{diag}\{\mathbf{h}_{IA}\}\mathbf{h}_{UI}$.

Proof: To find the optimal $\boldsymbol{\Theta}_A$, (11) can be converted to maximize the channel gain of U_A, i.e., $\mathbf{H}_A$. Define $\mathbf{U}_A^H = [e^{j\theta_A^1}, \cdots, e^{j\theta_A^M}]$. Then, the channel gain of U_A can be equivalent as

$$\begin{aligned}\mathbf{H}_A^{\theta*} &= \beta_A|\mathbf{U}_A^H\text{diag}\{\mathbf{h}_{IA}\}\mathbf{h}_{UI}|^2 \\ &= \beta_A|\mathbf{U}_A^H\mathbf{W}|^2 \overset{(a)}{=} \beta_A\left(\sum\nolimits_{m=1}^{M}|W_m|\right)^2,\end{aligned} \tag{13}$$

where (a) holds when (13) reaches its maximum, and $\theta_A^{m*} = \theta^* - \text{angle}\{W_m\}$ with θ^* an arbitrary value. ■

Then, we employ the semi-definite relaxation (SDR) to optimize the passive reflection beamforming of STAR-RIS $\boldsymbol{\Phi}_B$, which is equal to maximizing $\mathbf{H}_B$. Therefore, let $\mathbf{v} = \sqrt{\beta_B}[v_1, \cdots, v_M]^H$ and $\mathbf{L}_B = \text{diag}\{\mathbf{h}_{IB}\}\mathbf{h}_{UI}$, where $v_m = e^{j\theta_B^m}$ and $|v_m|^2 = 1$. As the equation $\mathbf{x}^H\boldsymbol{\Phi}\mathbf{y} = \phi^H\text{diag}\{\mathbf{x}^H\}\mathbf{y}$, we have $\mathbf{h}_{IB}\boldsymbol{\Phi}_B\mathbf{h}_{UI} = \mathbf{v}^H\mathbf{L}_B$. To obtain the optimal $\mathbf{v}$, we introduce an auxiliary variable u and have

$$\|\mathbf{h}_{IB}\boldsymbol{\Phi}_B\mathbf{h}_{UI}+h_{UB}\|^2=\|\mathbf{v}^H\mathbf{L}_B+h_{UB}\|^2=\bar{\mathbf{v}}^H\mathbf{X}\bar{\mathbf{v}}+\|h_{UB}\|^2, \tag{14}$$

where

$$\mathbf{X} = \begin{bmatrix} \mathbf{L}_B\mathbf{L}_B^H & \mathbf{L}_B h_{UB}^H \\ h_{UB}\mathbf{L}_B^H & 0 \end{bmatrix}, \bar{\mathbf{v}} = \begin{bmatrix} \mathbf{v} \\ u \end{bmatrix}. \tag{15}$$

Note that $\bar{\mathbf{v}}^H\mathbf{X}\bar{\mathbf{v}} = \text{tr}(\mathbf{X}\bar{\mathbf{v}}\bar{\mathbf{v}}^H)$, and we have

$$\mathbf{H}_B^{\mathbf{V}*} = \text{tr}(\mathbf{X}\mathbf{V}) + \|h_{UB}\|^2, \tag{16}$$

where $\mathbf{V} = \bar{\mathbf{v}}\bar{\mathbf{v}}^H$, and $\mathbf{V} \succeq 0$ and $\text{rank}(\mathbf{V}) = 1$ should be satisfied.

Accordingly, the simplified achievable rate of U_A and U_B can be given by

$$R_A' = \log_2\left(1 + p_A\beta_A\left(\sum\nolimits_{m=1}^{M}|W_m|\right)^2\Big/\sigma^2\right). \tag{17}$$

$$R_B' = \log_2\left(1 + \frac{p_B\mathbf{H}_B^{\mathbf{V}*}}{p_A\mathbf{H}_B^{\mathbf{V}*}+\sigma^2}\right). \tag{18}$$

Based on the above derivation, (11) can be converted into

$$\max_{\mathbf{V},\beta_i,p_i,} \quad R_A' + R_B' \tag{19a}$$

$$s.t. \quad (10c)-(10g), \tag{19b}$$

$$\mathbf{H}_A^{\theta*} \geq \mathbf{H}_B^{\mathbf{V}*}, \tag{19c}$$

$$\mathbf{V} \succeq 0, \tag{19d}$$

$$V_{n,n} = \beta_B, n = 1, \cdots, M, \tag{19e}$$

$$V_{M+1,M+1} = 1, \tag{19f}$$

$$\text{rank}(\mathbf{V}) = 1, \tag{19g}$$

where (19e) and (19f) enable the equality in (14).

However, it is still difficult to optimize the power allocation and transmission/reflection coefficients. To deal with (17), we introduce a slack variable t which satisfies $t^2 \leq p_A\beta_A$, resulting in $\|[2t, p_A - \beta_A]^H\| \leq p_A + \beta_A$. The lower bound of R_A' can be approximated by the first-order Taylor series as

$$R_A' \geq \log_2\left(1+(2t_0t-t_0^2)\left(\sum_{m=1}^{M}|W_m|\right)^2\Big/\sigma^2\right) \triangleq R_A^{lb}. \tag{20}$$

For R_B', it can be expressed with respect to p_A and $\mathbf{H}_B^{\mathbf{V}*}$ as

$$R_B' = \log_2(p\mathbf{H}_B^{\mathbf{V}*}+\sigma^2)-\log_2(p_A\mathbf{H}_B^{\mathbf{V}*}+\sigma^2) \triangleq R_B^1-R_B^2. \tag{21}$$

Considering that both p_A and $\mathbf{V}$ are variables in (21), an auxiliary variable $r \geq p_A\mathbf{H}_B^{\mathbf{V}*}$ is introduced. With the given local point $(p_{A0}, \mathbf{H}_{B0}^{\mathbf{V}*})$, its first-order Taylor expansion can be expressed as

$$r \geq \frac{1}{2}\Big[\left(p_{A0}+\mathbf{H}_{B0}^{\mathbf{V}*}\right)^2-2p_{A0}p_A+p_{A0}^2-2\mathbf{H}_{B0}^{\mathbf{V}*}\mathbf{H}_B^{\mathbf{V}*}+(\mathbf{H}_{B0}^{\mathbf{V}*})^2\Big]. \tag{22}$$

Accordingly, the lower bound of R_B based on the first-order Taylor expansion can be given by

$$R_B' \geq R_B^1-\left[\log_2(r_0+\sigma^2)+\frac{\log_2 e}{r_0+\sigma^2}(r-r_0)\right] \triangleq R_B^{lb}. \tag{23}$$

To handle the non-convex rank-one constraint (19g), we apply SDR to make it tractable. However, the obtained solution is an upper bound, which may not satisfy $\text{rank}(\mathbf{V}) = 1$. Hence, an additional step of Gaussian randomization is required to construct a rank-one solution, the details of which are omitted [18]. As a result, the reconfigured problem can be given by

$$\max_{\mathbf{V},\beta_i,p_i,t,r} \quad R_A^{lb} + R_B^{lb} \tag{24a}$$

$$s.t. \quad (10c)-(10e), \tag{24b}$$

$$R_A^{lb} \geq R_A(\gamma_A), \tag{24c}$$

$$R_B^{lb} \geq R_B(\gamma_B), \tag{24d}$$

$$\|[2t, p_A - \beta_A]^H\| \leq p_A + \beta_A, \tag{24e}$$

$$(19c)-(19f), (22), \tag{24f}$$

where the constraints (24c) and (24d) are the QoS requirements of users, which are equivalent to (10f) and (10g), respectively. Then, the problem (24) is convex and can be solved by CVX.

B. UAV Location Optimization

With the optimized variables in the last sub-section, the UAV location can be obtained by solving

$$\max_{\mathbf{Q}} \quad \log_2\left(1+\frac{p_A\mathbf{H}_A}{\sigma^2}\right)+\log_2\left(1+\frac{p_B\mathbf{H}_B}{p_A\mathbf{H}_B+\sigma^2}\right) \tag{25a}$$

$$s.t. \quad R_A \geq R_A(\gamma_A), \tag{25b}$$

$$R_B \geq R_B(\gamma_B), \tag{25c}$$

$$\mathbf{H}_A \geq \mathbf{H}_B, \tag{25d}$$

$$\mathbf{Q} \in \mathbf{L}. \tag{25e}$$

The objective function is neither convex nor concave. For brevity, we transform the channel gains of U_A and U_B into

$$\mathbf{H}_A = \|\mathbf{h}_{IA}\boldsymbol{\Phi}_A\mathbf{h}_{UI}\|^2 = \frac{\rho\|\mathbf{h}_{IA}\boldsymbol{\Phi}_A\tilde{\mathbf{h}}_{UI}\|^2}{d_{UI}^2} = \frac{A}{d_{UI}^2}, \tag{26}$$

$$\mathbf{H}_B = \|\mathbf{h}_{IB}\mathbf{\Phi}_B\mathbf{h}_{UI}+h_{UB}\|^2 = \frac{B}{d_{UI}^2}+\frac{C}{d_{UB}^{\alpha}}+\frac{2D}{d_{UI}d_{UB}^{\alpha/2}}, \quad (27)$$

where

$$A = \beta_A\rho^2M^2d_{IA}^{-2}, \quad (28a)$$
$$B = \rho\|\mathbf{h}_{IB}\mathbf{\Phi}_B\tilde{\mathbf{h}}_{UI}\|^2, \quad (28b)$$
$$C = \rho\|\tilde{h}\|^2, \quad (28c)$$
$$D = \rho Re\{\mathbf{h}_{IB}\mathbf{\Phi}_B\tilde{\mathbf{h}}_{UI}\tilde{h}^H\}. \quad (28d)$$

Note that the constraints (25b) and (25c) are difficult to handle due to their non-convexity, for which we apply successive convex approximation (SCA) on R_A and R_B as follows.

For R_A, the first-order Taylor expansion at the local point $\mathbf{Q}^k$ in the kth iteration can be given by

$$\begin{aligned} R_A &= \log_2\left(1+\frac{p_AA}{\|\mathbf{q}_I-\mathbf{Q}\|^2\sigma^2}\right) \\ &\geq \tilde{A}^k - \bar{A}^k\left(\|\mathbf{q}_I-\mathbf{Q}\|^2-\|\mathbf{q}_I-\mathbf{Q}^k\|^2\right) \triangleq R_A^{lb'}, \end{aligned} \quad (29)$$

where

$$\tilde{A}^k = \log_2\left(1+\frac{p_AA}{\|\mathbf{q}_I-\mathbf{Q}^k\|^2\sigma^2}\right), \quad (30)$$

$$\bar{A}^k = \frac{p_AA\log_2 e}{\left(p_AA+\sigma^2\|\mathbf{q}_I-\mathbf{Q}^k\|^2\right)\|\mathbf{q}_I-\mathbf{Q}^k\|^2}. \quad (31)$$

In order to tackle the non-convexity of R_B, we introduce two auxiliary variables z and s satisfying

$$z \leq \frac{p_B}{p_A+\frac{\sigma^2}{\mathbf{H}_B}}, \quad (32)$$

$$s \leq \frac{B}{d_{UI}^2}+\frac{C}{d_{UB}^{\alpha}}+\frac{2D}{d_{UI}d_{UB}^{\frac{\alpha}{2}}} = \widetilde{B}+\widetilde{C}+\widetilde{D}. \quad (33)$$

Accordingly, the achievable rate of U_B can be expressed as

$$\begin{aligned} R_B &= \log_2\left(1+\frac{p_B}{p_A+\sigma^2/\mathbf{H}_B}\right) \geq \log_2\left(1+\frac{p_B}{p_A+\sigma^2/s}\right) \\ &\geq \log_2(1+z) \triangleq R_B^{lb'}. \end{aligned} \quad (34)$$

However, (32) and (33) are non-convex. By the Taylor expansion at the given point z_0, (32) can be rewritten as

$$\sigma^2/s \leq p_B(1/z_0-(z-z_0)/z_0^2)-p_A, \quad (35)$$

To cope with (33), the three terms on the right side of the inequation are approximated separately. Since both B and C are positive, $\widetilde{B}$ and $\widetilde{C}$ are convex with d_{UI} and d_{UB}. Their lower bound can be expressed as the corresponding first-order Taylor series as

$$\widetilde{B} = Bd_{UI}^{-2} \geq B[3d_{UIk}^{-2}-2d_{UI}d_{UIk}^{-3}] \triangleq B_1, \quad (36)$$

$$\widetilde{C} = Cd_{UB}^{-\alpha} \geq C[(1+\alpha)d_{UBk}^{-\alpha}-\alpha d_{UB}d_{UBk}^{-\alpha-1}] \triangleq C_1, \quad (37)$$

where $d_{UIk} = \sqrt{\|\mathbf{q}_I-\mathbf{Q}^k\|^2}$ and $d_{UBk} = \sqrt{\|\mathbf{q}_B-\mathbf{Q}^k\|^2}$ denote the given local points in the kth iteration.

Nevertheless, it is not guaranteed that D is positive or negative due to different channel qualities. When $D>0$, the lower bound of $\widetilde{D}$ can be expressed as

$$\begin{aligned} \widetilde{D} &= 2Dd_{UI}^{-1}d_{UB}^{-\alpha/2} \geq 2D\Big[(2+\alpha/2)d_{UBk}^{-\alpha/2}d_{UIk}^{-1} \\ &-\alpha/2d_{UIk}^{-1}d_{UBk}^{-\frac{\alpha}{2}-1}d_{UB}-d_{UBk}^{-\alpha/2}d_{UIk}^{-2}d_{UI}\Big] \triangleq D_1^l, \end{aligned} \quad (38)$$

When $D<0$, we introduce two auxiliary variables $m \leq d_{UI}$ and $n \leq d_{UB}$, which can be written as $m^2 \leq \|\mathbf{q}_I-\mathbf{Q}\|^2$ and $n^2 \leq \|\mathbf{q}_B-\mathbf{Q}\|^2$, respectively. Considering that $\|\mathbf{q}_i-\mathbf{Q}\|^2$ is convex with the UAV location $\mathbf{Q}$, its lower bound approximated by the Taylor expansion can be given by

$$\|\mathbf{q}_i-\mathbf{Q}\|^2 \geq \|\mathbf{q}_i-\mathbf{Q}^k\|^2-2(\mathbf{q}_i-\mathbf{Q}^k)^T(\mathbf{Q}-\mathbf{Q}^k). \quad (39)$$

Accordingly, we have

$$m^2 \leq \|\mathbf{q}_I-\mathbf{Q}^k\|^2-2(\mathbf{q}_I-\mathbf{Q}^k)^T(\mathbf{Q}-\mathbf{Q}^k), \quad (40)$$

$$n^2 \leq \|\mathbf{q}_B-\mathbf{Q}^k\|^2-2(\mathbf{q}_B-\mathbf{Q}^k)^T(\mathbf{Q}-\mathbf{Q}^k). \quad (41)$$

The lower bound of $\widetilde{D}$ when $D \leq 0$ can be expressed as

$$\begin{aligned} \widetilde{D} &= 2Dd_{UI}^{-1}d_{UB}^{-\alpha/2} \geq D[(m^{-1}+n^{-\frac{\alpha}{2}})^2-m^2-n^{-\alpha}] \\ &\geq D\left[(m^{-1}+n^{-\frac{\alpha}{2}})^2-3m_0^{-2}+2m_0^{-3}m\right. \\ &\left.-(\alpha+1)n_0^{-\alpha}+\alpha n_0^{-\alpha-1}n\right] \triangleq D_1^g. \end{aligned} \quad (42)$$

Define a binary variable $flag$. When $D>0$, $flag=1$; otherwise, $flag=0$. The constraint (33) can be replaced by

$$s \leq B_1+C_1+flagD_1^l+(1-flag)D_1^g. \quad (43)$$

It is noted that we should approximate the constraint (25d) to make it convex, which can be expressed as

$$Ad_{UI}^{-2} \geq Bd_{UI}^{-2}+Cd_{UB}^{-\alpha}+2Dd_{UI}^{-1}d_{UB}^{-\frac{\alpha}{2}}. \quad (44)$$

Similar to the processing of $\widetilde{B}$, we have

$$Ad_{UI}^{-2} \geq A[3d_{UIk}^{-2}-2d_{UI}d_{UIk}^{-3}] \triangleq A_1. \quad (45)$$

Considering the constraint (33), (44) can be rewritten as

$$A_1 \geq s. \quad (46)$$

As a result, the sub-problem of UAV's location can be transformed into a convex one as

$$\max_{\mathbf{Q},s,z,m,n} \quad R_A^{lb'}+R_B^{lb'} \quad (47a)$$
$$s.t. \quad \mathbf{Q} \in \mathbf{L}, \quad (47b)$$
$$(35),(40),(41),(43),(46), \quad (47c)$$

which can be solved by CVX.

C. Algorithm Design

Based on the above derivations, we propose an iterative algorithm, which is summarized in Algorithm 1. In particular, (11) and (25) are solved iteratively until convergence. Define $R_o(p_i^{(k-1)},\beta_i^{(k-1)},\mathbf{\Theta}_i^{(k-1)},\mathbf{Q}^{(k-1)})$ as the objective value of (10). After Step 4, we have $R_o(p_i^{(k-1)},\beta_i^{(k-1)},\mathbf{\Theta}_i^{(k-1)},\mathbf{Q}^{(k-1)}) \leq R_o(p_i^{(k)},\beta_i^{(k)},\mathbf{\Theta}_i^{(k)},\mathbf{Q}^{(k-1)})$, where the objective value of (24) is a lower bound of (11) and the approximation is tight at the optimal points. Similarly, we obtain $R_o(p_i^{(k)},\beta_i^{(k)},\mathbf{\Theta}_i^{(k)},\mathbf{Q}^{(k-1)}) \leq R_o(p_i^{(k)},\beta_i^{(k)},\mathbf{\Theta}_i^{(k)},\mathbf{Q}^{(k)})$ by Step 6. Therefore, the objective value of (10) is non-decreasing over iterations. In addition, the optimal value of

(10) is upper bounded by a finite value. Thus, Algorithm 1 is guaranteed to converge. Denote K as the number of iterations required for convergence. In each iteration, the problems (24) and (47) are solved alternatively. According to the analysis in [19], the total computational complexity of Algorithm 1 can be given by $\mathcal{O}(KM^{6.5})$.

Algorithm 1 Iterative Algorithm for Problem (10)

1: **Initialization**: Initialize p_i^0, β_i^0, $\mathbf{V}_0$, $\mathbf{Q}_0$, t_0, r_0, s_0 and z_0. Set the iteration number $k = 0$;
2: **repeat**
3: With given $\mathbf{Q}_k$, calculate the optimal $\mathbf{\Theta_A}$ with (12).
4: With given $\mathbf{Q}_k$ and $\mathbf{\Theta_A}$, solve the problem (24) and update p_i^k, β_i^k, $\mathbf{V}_k$, t_k and r_k;
5: Find $\mathbf{\Theta}_B^k$ with Gaussian randomization and obtain $\mathbf{\Phi}_i^k = \sqrt{\beta_i^k}\mathbf{\Theta}_i^k$;
6: With given $\mathbf{\Phi}_i^k$ and p_i^k, update $\mathbf{Q}_k$ by solving the problem (47);
7: Calculate the sum rate by utilizing (6) and (7);
8: Set $k = k + 1$;
9: **until** : Convergence.

D. Multi-user Scenario

The proposed scheme can be extended to a multi-user case after incorporating proper kind of multiple access and can be solved similarly. Specifically, the users can be divided into J groups, each of which consists of two users on both sides of STAR-RIS, served via NOMA. In this case, the closed-form solution to the transmission phase shifts is not applicable and the sum transmit power in each pair should be optimized. To handle this problem, we divide it into three subproblems and optimize the variables $\{\mathbf{\Phi}_A, \mathbf{\Phi}_B\}$, $p_{i,j}$ and $\mathbf{Q}$ alternately until convergence, where $p_{i,j}$ is the transmit power for the i-th user in the j-th group, $j = \{1, 2, \cdots, J\}$. Specifically, we first optimize the transmission beamforming by using SDR similarly to the reflection beamforming. Then, for the power allocation problem, the objective function can be rewritten similarly to (17) and (21), and its lower bound can be obtained based on the first-order Taylor expansion. Finally, the UAV location optimization in the multi-user case can be solved by referring to (47).

V. Simulation Results

Simulation results are presented to demonstrate the effectiveness of the proposed scheme. We set $\rho = -20$ dB, $\sigma^2 = -90$ dBm and $\alpha = 3.8$. The total transmit power, the number of STAR-RIS elements and the QoS requirement of users are set as 10 mW, 36 and 2 bit/s/Hz, if not specified [20]. The QoS requirements of U_A and U_B are assumed to be equal. Assume that the UAV hovers at $H = 100$ m in the area $\mathbf{L}$. U_A, U_B and STAR-RIS are assumed to be located at $\mathbf{q}_A = [10, -5, 30]$ m, $\mathbf{q}_B = [50, 50, 0]$ m and $\mathbf{q}_I = [20, 0, 30]$ m, respectively.

Fig. 2 presents the sum rate versus the number of STAR-RIS reflecting elements M. For performance comparison, several

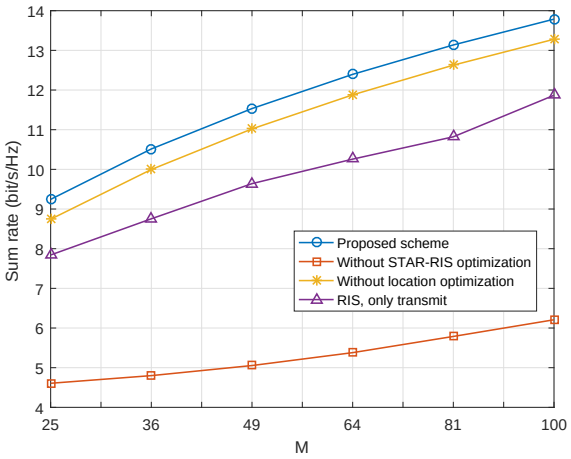

Fig. 2. Sum rate versus the number of STAR-RIS reflecting elements.

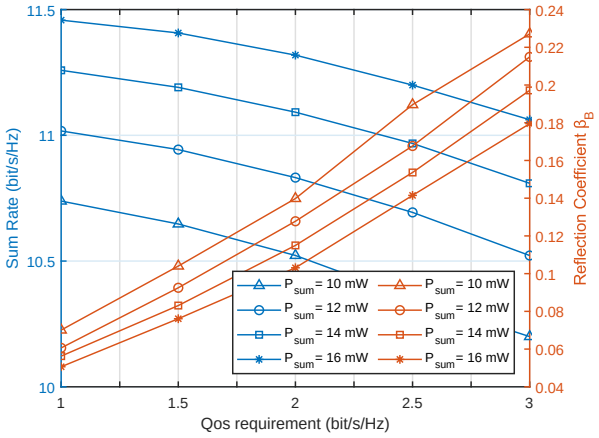

Fig. 3. Sum rate and reflection coefficients versus the QoS requirement.

benchmarks are considered. The benchmark "Without STAR-RIS optimization" shows the sum rate when applying random phase shifts. "Without location optimization" performs the power allocation and phase shifts design with the fixed UAV location. "RIS, only transmit" indicates the performance when the elements of RIS only transmit to U_A, and U_B in the reflection side can only receive the signal from the direct link. It can be observed that the achievable rate increases with M for all the schemes. This is because with a larger RIS size, better passive beamforming gain can be achieved for users. Due to the optimization limitations, different schemes have different effects on the sum rate. The performance of the proposed scheme is much better than that of the benchmarks, due to the joint optimization. Their gaps indicate the advantages of the optimization of UAV location, the full coverage and the beamforming of STAR-RIS, respectively.

In Fig. 3, we present the sum rate and the reflection coefficient β_B of U_B versus the QoS requirement. As expected, the sum rate/reflection coefficient increases/decreases with the total transmit power P_{sum}, as higher signal-to-noise ratio (SNR) can be achieved. In addition, it can be observed that the sum rate decreases with γ and the reflection coefficient increases with γ. The reason is that with lower QoS requirement, more degree of freedom can be obtained for the power allocation and transmission/reflection coefficient design, which leads to

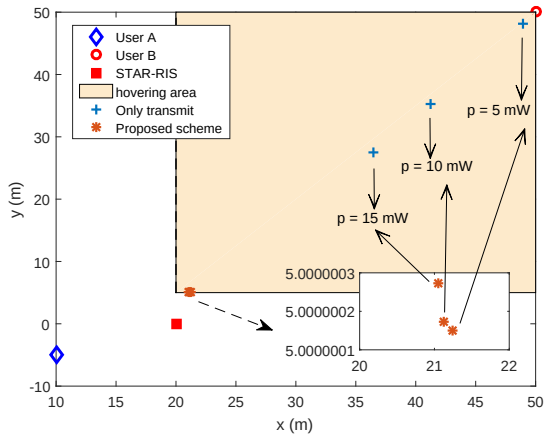

Fig. 4. Optimal UAV's location with different transmit power in the proposed scheme and the benchmark.

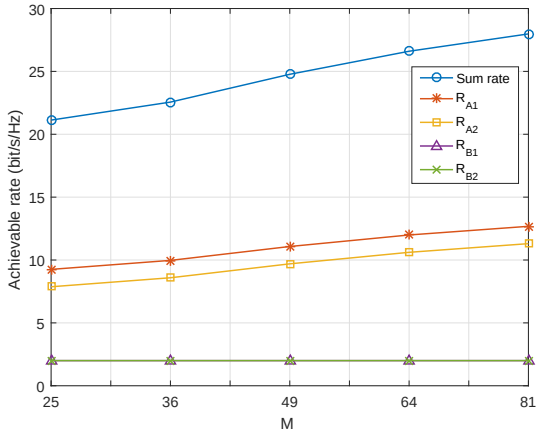

Fig. 5. Achievable rate versus the number of STAR-RIS reflecting elements in a multi-user scenario, with four users and $J = 2$.

a higher sum rate and a smaller reflection coefficient.

Fig. 4 depicts the optimal location of UAV for different transmit power in the proposed scheme and benchmarks. From the results, it can be seen that in the case "RIS, only transmit", the optimal location gets closer to the weak user U_B as the transmit power p decreases. However, the optimal location is almost unchanged in the proposed scheme, which are close to the RIS to reduce the path loss. This is because when p changes, the achievable rate of weak user U_B can be ensured by adjusting the reflection coefficient β_B, which shows the effectiveness of joint optimization of transmission/reflection coefficient, phase shifts, power allocation and UAV location.

For the multi-user scenario, we set the total transmit power to 0.1 W. Fig. 5 shows the achievable rate of the users versus the number of STAR-RIS elements. It can be observed that the sum rate increases with M. However, the achievable rate of reflection users consistently just meets their QoS requirements. This is because it tends to allocate more resource to the interference-free user to increase the sum rate.

VI. Conclusion

In this correspondence, we have investigated the sum-rate maximization in STAR-RIS assisted NOMA-UAV networks, where the location of UAV, the transmit power and the transmission/reflection beamforming of STAR-RIS are jointly optimized. The problem is decomposed into two sub-problems, and the non-convex constraints are transformed into convex via SCA. Then, an iterative algorithm is developed to optimize the two subproblems alternatively. Simulation results show the effectiveness of the proposed iterative algorithm.

References

[1] Q. Wu, S. Zhang, B. Zheng, C. You, and R. Zhang, "Intelligent reflecting surface-aided wireless communications: A tutorial," *IEEE Trans. Commun.*, vol. 69, no. 5, pp. 3313–3351, May 2021.

[2] Q. Wu and R. Zhang, "Towards smart and reconfigurable environment: Intelligent reflecting surface aided wireless network," *IEEE Commun. Mag.*, vol. 58, no. 1, pp. 106–112, Jan. 2020.

[3] X. Yu, D. Xu, Y. Sun, D. W. K. Ng, and R. Schober, "Robust and secure wireless communications via intelligent reflecting surfaces," *IEEE J. Sel. Areas Commun.*, vol. 38, no. 11, pp. 2637–2652, Nov. 2020.

[4] Y. Zeng, Q. Wu, and R. Zhang, "Accessing from the sky: A tutorial on UAV communications for 5G and beyond," *Proc. IEEE*, vol. 107, no. 12, pp. 2327–2375, Dec. 2019.

[5] J. Wang, B. Li, G. Wang, Y. Hu, and A. Schmeink, "Robust design for UAV-enabled multiuser relaying system with SWIPT," *IEEE Trans. Green Commun. Netw.*, vol. 5, no. 3, pp. 1293–1305, Mar. 2021.

[6] X. Yuan, Y. Hu, D. Li, and A. Schmeink, "Novel optimal trajectory design in UAV-assisted networks: A mechanical equivalence-based strategy," *IEEE J. Sel. Areas Commun.*, vol. 39, no. 11, pp. 3524–3541, Nov. 2021.

[7] X. Pang, M. Sheng, N. Zhao, J. Tang, D. Niyato, and K.-K. Wong, "When UAV meets IRS: Expanding air-ground networks via passive reflection," *IEEE Wirel. Commun.*, vol. 28, no. 5, pp. 164–170, May 2021.

[8] C. Wang, X. Chen, J. An, Z. Xiong, C. Xing, N. Zhao, and D. Niyato, "Covert communication assisted by UAV-IRS," *IEEE Trans. Commun.*, vol. 71, no. 1, pp. 357–369, Jan. 2023.

[9] X. Pang, N. Zhao, J. Tang, C. Wu, D. Niyato, and K.-K. Wong, "IRS-assisted secure UAV transmission via joint trajectory and beamforming design," *IEEE Trans. Commun.*, vol. 70, no. 2, pp. 1140–1152, Feb. 2022.

[10] H. Mei, K. Yang, Q. Liu, and K. Wang, "3D-trajectory and phase-shift design for ris-assisted UAV systems using deep reinforcement learning," *IEEE Trans. Veh. Technol.*, vol. 71, no. 3, pp. 3020–3029, Mar. 2022.

[11] H. Lu, Y. Zeng, S. Jin, and R. Zhang, "Aerial intelligent reflecting surface: Joint placement and passive beamforming design with 3D beam flattening," *IEEE Trans. Wireless Commun.*, vol. 20, no. 7, pp. 4128–4143, Jul. 2021.

[12] J. Xu, Y. Liu, X. Mu, and O. A. Dobre, "STAR-RISs: Simultaneous transmitting and reflecting reconfigurable intelligent surfaces," *IEEE Commun. Lett.*, vol. 25, no. 9, pp. 3134–3138, Sep. 2021.

[13] H. Zhang, S. Zeng, B. Di, Y. Tan, M. Di Renzo, M. Debbah, Z. Han, H. V. Poor, and L. Song, "Intelligent omni-surfaces for full-dimensional wireless communications: Principles, technology, and implementation," *IEEE Commun. Mag.*, vol. 60, no. 2, pp. 39–45, Feb. 2022.

[14] Y. Liu, B. Duo, Q. Wu, X. Yuan, and Y. Li, "Full-dimensional rate enhancement for UAV-enabled communications via intelligent omni-surface," *IEEE Wireless Commun. Lett.*, vol. 11, no. 9, pp. 1955–1959, Sep. 2022.

[15] Q. Zhang, Y. Zhao, H. Li, S. Hou, and Z. Song, "Joint optimization of STAR-RIS assisted UAV communication systems," *IEEE Wireless Commun. Lett.*, vol. 11, no. 11, pp. 2390–2394, Nov. 2022.

[16] Z. Wang, X. Mu, Y. Liu, and R. Schober, "Coupled phase-shift STAR-RISs: A general optimization framework," *IEEE Wireless Commun. Lett.*, vol. 12, no. 2, pp. 207–211, Feb. 2023.

[17] C. Wu, C. You, Y. Liu, X. Gu, and Y. Cai, "Channel estimation for STAR-RIS-aided wireless communication," *IEEE Commun. Lett.*, vol. 26, no. 3, pp. 652–656, Mar. 2022.

[18] Q. Wu and R. Zhang, "Intelligent reflecting surface enhanced wireless network via joint active and passive beamforming," *IEEE Trans. Wireless Commun.*, vol. 18, no. 11, pp. 5394–5409, Nov. 2019.

[19] K.-Y. Wang, A. M.-C. So, T.-H. Chang, W.-K. Ma, and C.-Y. Chi, "Outage constrained robust transmit optimization for multiuser MISO downlinks: Tractable approximations by conic optimization," *IEEE Trans. Signal Process.*, vol. 62, no. 21, pp. 5690–5705, 2014.

[20] S. Li, B. Duo, X. Yuan, Y.-C. Liang, and M. Di Renzo, "Reconfigurable intelligent surface assisted UAV communication: Joint trajectory design and passive beamforming," *IEEE Wireless Commun. Lett.*, vol. 9, no. 5, pp. 716–720, May 2020.